Theor Chem Account (2008) 120:395–403
DOI 10.1007/s00214-008-0422-y

REGULAR ARTICLE

Theoretical study of the gas-phase ethane C–H and C–C bonds activation by bare niobium cation

M. C. Michelini · I. Rivalta · E. Sicilia

Received: 23 October 2007 / Accepted: 6 February 2008 / Published online: 29 February 2008

Abstract The potential energy surfaces for the reaction of bare niobium cation with ethane, as a prototype of the C–H and C–C bonds activation in alkanes by transition metal cations, have been investigated employing the Density Functional Theory in its B3LYP formulation. All the minima and key transition states have been examined along both high- and low-spin surfaces. For both the C–H and C–C activation pathways the rate determining step is that corresponding to the insertion of the Nb cation into C–H and C–C bond, respectively. However, along the C–H activation reaction coordinate the barrier that is necessary to overcome is 0.13 eV below the energy of the ground state reactants asymptote, while in the C–C activation branch the corresponding barrier is about 0.58 eV above the energy of reactants in their ground state. The overall calculated reaction exothermicities are comparable. Since the spin of the ground state reactants is different from that of both $H–Nb^+–C_2H_5$ and $CH_3–Nb^+–CH_3$ insertion intermediates and products, spin multiplicity has to change along the reaction paths. All the obtained results, including Nb^+–R binding energies for R fragments relevant to the examined PESs, have been compared with existing experimental and theoretical data.

Keywords Alkane activation · PES · Spin crossing · DFT

Contribution to the Nino Russo Special Issue.

M. C. Michelini · I. Rivalta · E. Sicilia (✉)
Dipartimento di Chimica and Centro di Calcolo
ad AltePrestazioni per Elaborazioni Parallele e
Distribuite-Centro d'Eccellenza MURST,
Università della Calabria,
87030 Arcavacata di Rende, Italy
e-mail: siciliae@unical.it

1 Introduction

Activation of methane and alkanes by transition metals has been a topic of growing interest during the past decades, due to economic interest in alkanes conversion and chemistry [1–3]. In spite of the important recently made progress in this field many questions are still open and further efforts have to be made to understand the fundamental prerequisites for the activation process. From this viewpoint it is mostly important to individuate which transition metals are the most suitable for this purpose.

One way to accomplish the aim to unravel the intrinsic reactivities of transition metals is to use gas-phase techniques. The possibility to perform experimental gas-phase studies on "isolated" reactants has been increased in the last years with the advent of new mass-spectrometric techniques that allow the generation of mass-selected, ground state electronic species and to explore their chemistry under well-defined conditions. The fruitful interplay between such experimental studies and high-level theoretical investigations of the transition metals reactivity in gas-phase has provided deep insights into the elementary steps of catalytic processes, reactivity patterns, importance of the electronic structure, nature of intermediates and role of ligation [4]. Detailed investigations have been carried out, indeed, on the influence of the addition of ligands, oxo ligands in particular, on the reactivity of the bare metal cations [5–7].

The involvement of transition metals makes the situation particularly intriguing due to the ability of the metal center to access multiple low-lying electronic states and to adapt to different bonding situations, which may enable the system to find low-energy reaction paths not accessible otherwise. Then, spin crossing between surfaces of different multiplicities can occur during the reaction and products formation arises from an interplay between spin inversion,

barrier height, and thermodynamic factors. The idea of state-selective reactivity has been introduced, at first, by Armentrout and co-workers [8,9] and the role of spin flip in organometallic chemistry has been underlined by the introduction of the so-called two state reactivity (TSR) paradigm [10]. In more recent years, a careful level of attention has been devoted to the involved potential energy surfaces and the regions where they cross and new computational techniques have been introduced that help to understand the situation [11–13].

In the framework of a more extended project [14–20] aiming to unravel the mechanistic details of catalytic processes for the activation of prototypical bonds mediated by transition metal containing systems, we have carried out the study of the reaction of the niobium cation with ethane, which is the simplest alkane molecule in which both C–C and C–H bond can be activated. Density functional theory (DFT) has been applied to characterize all the minima and first-order saddle points and to present a complete mechanistic scheme of the reaction. Both quintet and triplet PESs have been examined in accordance with TSR paradigm. Bond dissociation energies (BDEs) for Nb^+–R fragments have been calculated and compared with recently [21] and less recently [22–24] experimentally determined values and previous theoretical [25–34] calculations.

The reaction mechanism for the activation of both C–C and C–H bond has been studied according to the general scheme proposed for these kinds of reactions that involves as the first step the formation of a metal–ligand adduct followed by oxidative insertion of the metallic center into one bond of the ligand molecule. Formation of this first insertion intermediate is very often the key step of the process since the ground state of the intermediate could not correspond to the ground state of the metal. The next steps are migration of one or more atoms or groups of the ligand molecule to the metal and reductive elimination of a small molecule provided that intermediates have sufficiently high lifetimes to undergo rearrangements. Bond breakings that are generally not accessible at thermal energies become dominant at high energies. Results have been compared with the hypotheses on the reaction mechanism proposed on the basis of experimental results [21].

2 Computational details

Geometry optimizations as well as frequency calculations for all the reactants, intermediates, products and transition states were performed at the Density Functional level of theory, employing the Becke's three-parameter hybrid functional [35] combined with the Lee, Yang and Parr (LYP) [36] correlation functional, denoted as B3LYP within the GAUSSIAN03 package [37].

The LANL2DZ effective core potential [38–40] has been used for the metal center. In LANL2DZ, the valence shell are explicitly represented using a double zeta and the valence electrons considered for the transition metal are $4s^2 4p^6 4d^4 5s^1$. The standard 6-311+G(2df,2p) basis sets [41,42] have been employed for the rest of the atoms.

No symmetry restrictions have been imposed during the geometry optimizations, whereas for each optimized stationary point vibrational analysis has been performed to determine its character (minimum or saddle point) and to evaluate the zero-point vibrational energy (ZPVE) corrections, which are included in all relative energies. For all the reported transition states it has been carefully checked that the vibrational mode associated to the imaginary frequency corresponds to the correct movement of involved atoms. All the minima connected by a given transition state were confirmed by intrinsic reaction coordinate (IRC) calculations [43,44] (in mass-weighted coordinates) as implemented in GAUSSIAN03 program.

For all the studied species we have checked $\langle S^2 \rangle$ values to evaluate whether spin contamination can influence the quality of the results. In all cases we have found that the calculated values differ from $S(S+1)$ by less that 10%.

The counterpoise corrections have been calculated to correct bond dissociation energies for basis set superposition error (BSSE) [45]. A full natural bond orbital (NBO) analysis [46,47] of all the cationic Nb–R^+ fragments has been performed to give further insight into their bonding properties.

3 Results and discussion

The most reliable source of experimental information on the Nb^+ + ethane reaction is the guided ion beam mass spectrometry study by Armentrout and co-workers [21] although the same system has been also examined in a previous ion cyclotron resonance study by Freiser and coworkers [48]. Ground state Nb^+ ions are found to be very reactive with ethane over a wide range of kinetic energies. At low energies the dominant process is the dehydrogenation reaction, whose cross section is consistent with an exothermic reaction having no barriers in excess of the reactants energy. At higher energies other products become accessible and the dominant process is C–H bond cleavage to form NbH^+ and C_2H_5. For the C–C bond activation the authors indicate that the lowest energy product formed by cleavage of the C-C bond is $NbCH_2^+$ together with methane and the cross section for the formation of this product is characteristic of an inefficient near-thermoneutral process.

The computed B3LYP potential energy surfaces for the C–H activation branch of the reaction on Nb^+ with C_2H_6 are shown in Fig. 1 and the corresponding most relevant geometrical parameters for minima and transition states along high- and low-spin PESs are reported in Fig. 2.

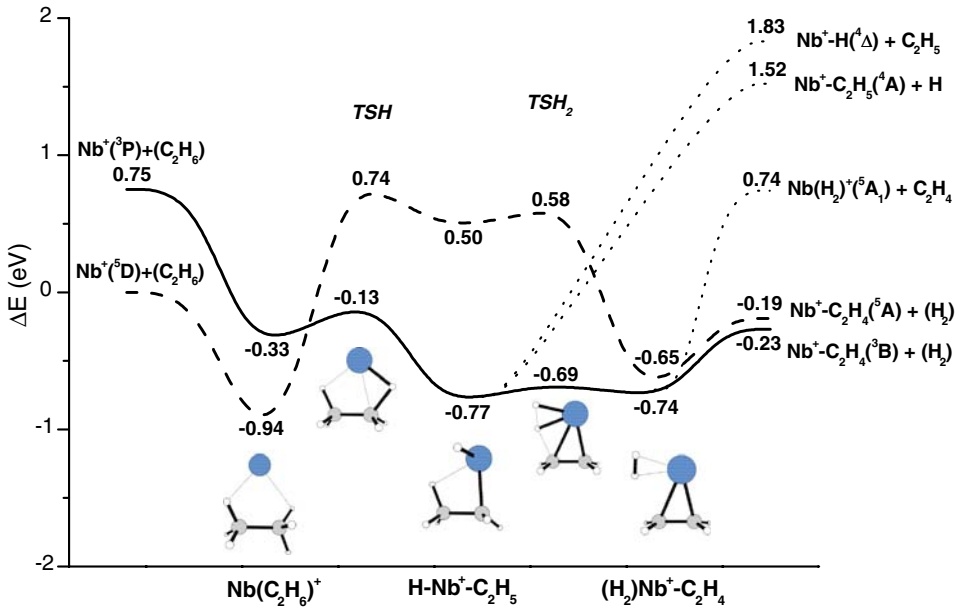

Fig. 1 Quintet and triplet PESs for the C–H activation branch of the reaction of Nb^+ bare cation with C_2H_6. Energies are in eV and relative to the ground-state reactants

The PESs theoretically predicted for the interaction of the niobium cation with the C–C bond are sketched in Fig. 3, while geometrical parameters of stationary points are collected in Fig. 4.

Relative energies for both reaction branches are calculated with respect to the reactants asymptote represented by the metal center in its ground state configuration and the ethane molecule. The ground state of the Nb cation is of ^5D symmetry and arises from the $4d^4$ configuration, while the first triplet ^{3}P excited state, corresponding to the $4d^4$ configuration lies 0.83 eV above [49]. The theoretical value obtained by us, 0.75 eV, is underestimated by only 0.08 eV.

3.1 C–H bond activation

The first step of the dehydrogenation reaction of ethane by bare Nb cation, as shown in Fig. 1, is the exothermic formation of a $Nb(C_2H_6)^+$ complex along both high- and low-spin PESs. The ^{5}A ground state of the ion–molecule complex, $Nb(C_2H_6)^+$, is calculated to be more stable than the reactants asymptote by 0.94 eV. The corresponding ^{3}A complex lies 0.61 eV above. In both quintet and triplet $Nb(C_2H_6)^+$ adducts the ethane structure has retained the staggered conformation of the isolated molecule, and the niobium cation is perfectly located above the center of the C–C bond with Nb distances of 2.544 and 2.502 Å for quintet and triplet, respectively. The reaction proceeds to form the insertion intermediate H–Nb^+–C_2H_5 through the first order saddle point TSH in which the niobium cation has been inserted into one of the C–H bonds. The low spin triplet TSH lies lower in energy than the corresponding high spin state and 0.13 eV below the energy of the ground state reactants. It has one imaginary frequency of 1,098i cm^{-1}, which mainly corresponds to the expected movement of the hydrogen atom detaching from the carbon atom and moving toward Nb. The quintet TSH lies 0.74 eV above the reactants asymptote and the transition vector corresponding to its imaginary frequency of 342i cm^{-1} describes the movements of all the atoms participating to the isomerization. Its geometry is already close to the C–H inserted species, that is very product like because the quintet H–Nb^+–C_2H_5 complex is much less stable than the corresponding initial ion–molecule adduct. Since the ground state multiplicity of TSH is different with respect to ground state spin multiplicity of reactants, an intersystem crossing from the quintet to the triplet surface has to take place in this region of the PES. On the basis of the present results this crossing occurs at an energy below that of the separated reactants and spin–orbit coupling should be large enough to allow for an efficient conversion to the energetically favored surface as it has already been concluded examining experimental data [21].

The H–Nb^+–C_2H_5 intermediate resulting from the C–H insertion process is more stable in a triplet low-spin state as two of the valence electrons of the metal are involved in the formation of H–Nb and Nb–C covalent bonds and lies 0.77 eV below the ground state reactants. This intermediate is stabilized (by about 0.18 eV) by a kind of β-agostic interaction through the appropriate hydrogen at the adjacent methyl group. The presence of this agostic interaction is evidenced by the elongation of the C–H bond (1.158 Å) and the reduction of the HCC bond angle (111.7°). The corresponding quintet intermediate is much less stable and does not profit from such an agostic interaction.

Following the C–H bond insertion, the reaction proceeds through a second intramolecular rearrangement to yield a

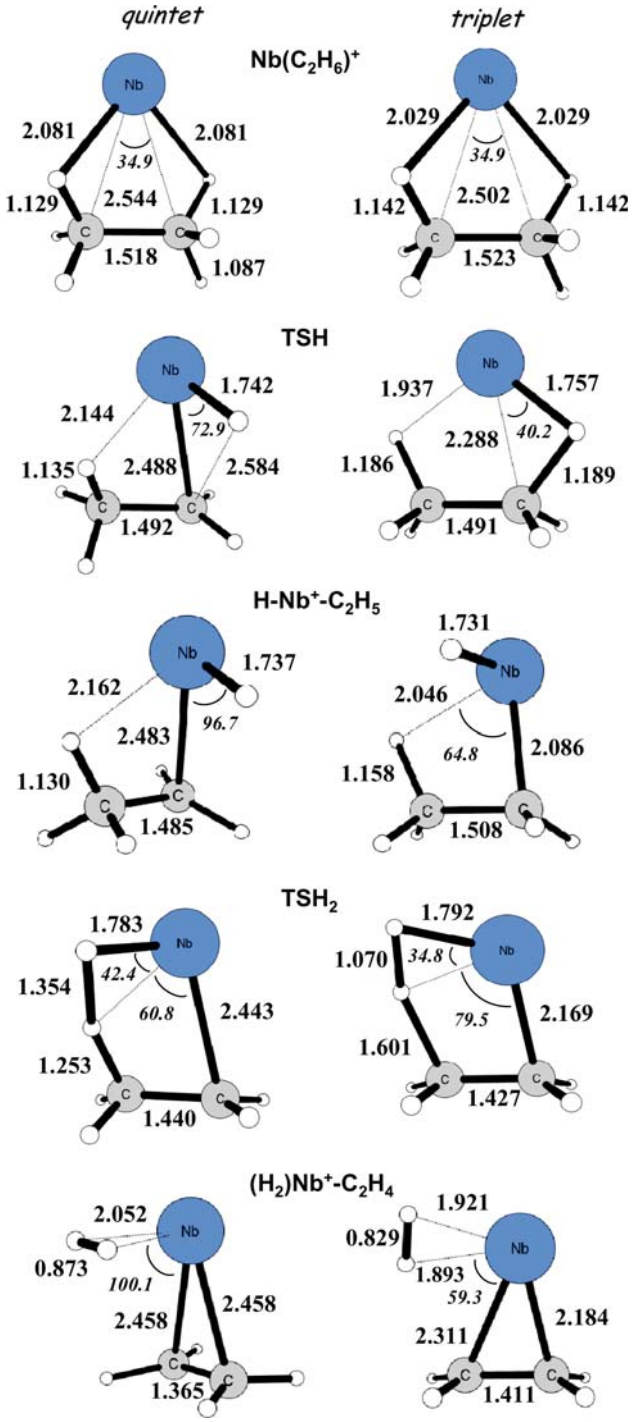

Fig. 2 Optimized geometries of calculated minima and transition states along the quintet and triplet PESs for the ethane C–H bond activation by Nb^+. Bond lengths are in angstroms and angles in degrees

new intermediate that may be either a complex, in which the niobium–ethylene cation is complexed by molecular hydrogen, $(H_2)Nb^+–C_2H_4$, or a covalently bonded dihydrido complex, $HH–Nb^+–C_2H_4$, obtained by direct hydrogen transfer from carbon atom to the metal center. The possibility that a covalently bonded intermediate is formed has not ruled out a priori but since all the attempts carried out to localize a minimum, $HH–Nb–C_2H_4$, corresponding to a direct β-hydrogen transfer to the metal have failed it can be reasonably concluded that the dihydrido species does not exist as a minimum along the dehydrogenation pathway.

The $(H_2)Nb^+–C_2H_4$ intermediate is obtained through a concerted four-center elimination of H_2 corresponding to the TSH_2 transition state characterized by an almost-fully formed H–H bond and an imaginary frequency of $949i$ cm^{-1} corresponding to expected movements of the involved atoms that confirm the concerted nature of this H_2 activation saddle point. The energy of the triplet TSH_2 structure, localized well below the reactants asymptote, differs by only 0.05 eV from that of the final ion–molecule complex.

The triplet $(H_2)Nb^+–C_2H_4$ complex is characterized by an electrostatic interaction between the cationic niobium–ethylene complex and molecular hydrogen, while the structure of the $Nb^+–C_2H_4$ moiety is very close to that of the final product, obtained by elimination of molecular hydrogen, although the interaction of niobium ion with carbon atoms is unsymmetrical yet.

The last step of the reaction, the formation of the dehydrogenation products, takes place directly from intermediate $(H_2)Nb^+–C_2H_4$, without an energy barrier and hydrogen release is endothermic by 0.51 eV. The overall process results to be exothermic by about 0.23 eV. The comprehensive picture of the reaction that can be drawn on the basis of our computations is that once the system accesses the triplet reaction coordinate via a curve crossing in the region of the transition state corresponding to the first hydrogen shift from carbon to niobium, dehydrogenation products are very fast formed.

The possible alternative process to yield from the same $(H_2)Nb^+–C_2H_4$ intermediate the neutral alkene molecule, is calculated to be endothermic by 0.74 eV, in agreement with the measured threshold of 1.04 ± 0.19 eV [21], and represents the only way to generate the $Nb(H_2)^+$ fragment.

The $H–Nb^+–C_2H_5$ intermediate, instead, is an obvious choice for the formation of NbH^+ and $NbC_2H_5^+$ fragments that can be obtained by simple Nb–C and Nb–H bond breaking. Figure 1 shows as formation of these fragments is endothermic by 1.83 eV for the former and 1.52 eV for the latter. The predicted threshold for the NbH^+ product is 2.03 ± 0.07 eV [21], while the measured threshold is even higher (2.36 ± 0.19 eV) apparently due to the competition with the more favorable dehydrogenation process. When the energy barrier associated to a tight transition state involving complicated rearrangements is high it should be very plausible that at high kinetic energies simple bond breaking processes, even entropically favored, become competitive. However, for the situation examined here the barrier associated to the TSH_2 transition state lies well below the

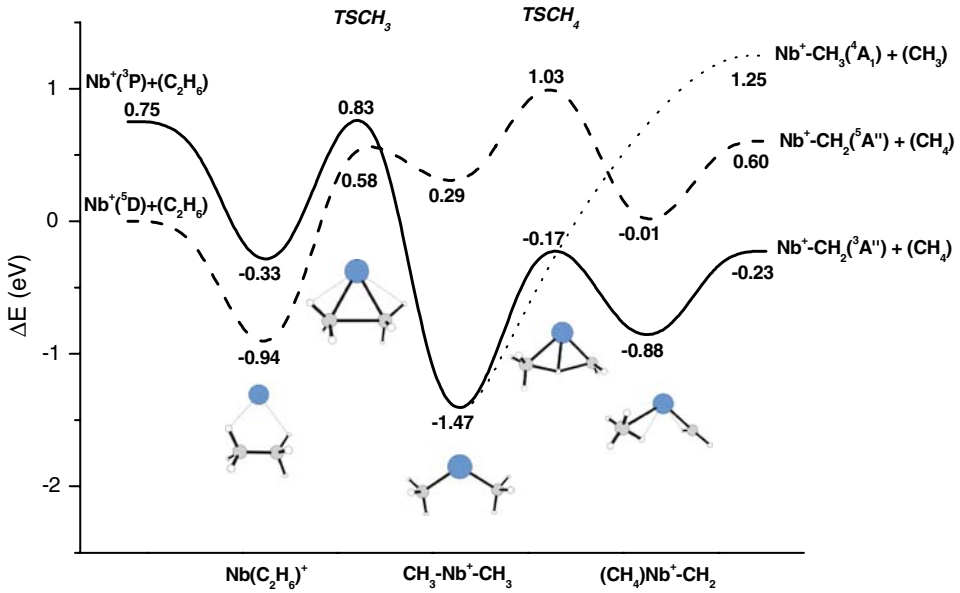

Fig. 3 Quintet and triplet PESs for the C–C activation branch of the reaction of Nb^+ bare cation with C_2H_6. Energies are in eV and relative to the ground-state reactants

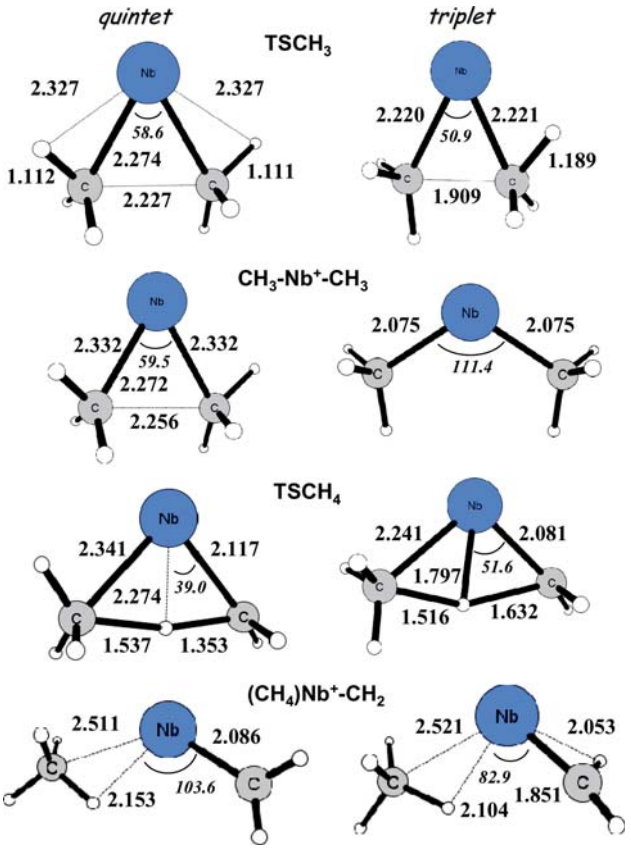

Fig. 4 Optimized geometries of calculated minima and transition states along the quintet and triplet PESs for the ethane C–C bond activation by Nb^+. Bond lengths are in angstroms and angles in degrees

reactants asymptote and its height is so low (only 0.08 eV) that the dehydrogenation process dominates even at high kinetic energies.

3.2 C–C bond activation

Let us now turn to the alternative C–C activation branch of the reaction of niobium ion with ethane. As it is shown in Fig. 3, the initial $Nb(C_2H_6)^+$ complex is common to both branches, which then fork into the C–H activation pathway through the TS_H transition state and the C–C bond activation regime via the $TSCH_3$ transition state (see Fig. 3). This saddle point in its quintet multiplicity is located at 0.58 eV above the $Nb^+(^5D) + C_2H_6$ asymptote and is characterized as a transition state by only one imaginary frequency of $77i$ cm^{-1}, corresponding to the breaking of the C–C bond and rotation of the CH_3 groups toward Nb^+. Quintet $TSCH_3$ structure is 0.83 eV higher in energy of the ground state reactants and is analogously characterized by only one imaginary frequency. The insertion of Nb^+ into the C–C bond yields the inserted dimethyl intermediate, CH_3–Nb^+–CH_3. The formation of two Nb–C covalent bonds as the outcome of the pairing of two metal electrons with two electrons of the CH_3 ligands is responsible for the enhanced stability of the triplet structure of the CH_3–Nb^+–CH_3 intermediate that, indeed, lies 1.47 eV below the reactants asymptote. The corresponding quintet structure lies 0.29 eV above reactants ground state. Our results are in qualitative agreement with those reported in a former study by Rosi et al. [33] that have found the dimethyl ion to adopt a bent structure and to be more stable than the electrostatic $Nb(C_2H_6)^+$ complex. However, from our calculations formation of dimethyl complex results to be much more exothermic and the energy difference between the two isomers more pronounced.

Since the ground state of the CH_3–Nb^+–CH_3 insertion complex has only two unpaired electrons with respect to reactants quintet ground state, a crossing from the quintet to the

triplet PES takes place after passage of the quintet $TSCH_3$ transition state, even if such a kind of spin crossover is not considered a rate limiting factor as it involves species with excess energy [10].

The reaction proceeds along the triplet pathway to convert the dimethyl intermediate into another stable ion–molecule complex, $(CH_4)Nb^+–CH_2$, which serves as the direct precursor for loss of methane. This structure contains a slightly distorted η^3 methane molecule bound (Nb–C distance is 2.521 Å) to the niobium carbene cation, which shows a typical Nb–H distance of 2.053 Å. The triplet $(CH_4)Nb^+–CH_2$ complex is calculated to lie 0.88 eV below the reactants dissociation limit, while formation of the corresponding quintet is calculated to be nearly thermoneutral.

The triplet first order saddle point $TSCH_4$ for the 1,3 hydrogen shift that directly converts the dimethyl complex into the $(CH_4)Nb^+–CH_2$ cation is characterized by an imaginary frequency of $1{,}348i$ cm^{-1} and the normal mode associated to it clearly identifies the hydrogen shift from one methyl to the other. The relative energy of $TSCH_4$ with respect to the reactants and the dimethyl complex is −0.17 and 1.30 eV, respectively. The structure of this transition state shows one of the Nb–C distances elongated by about 0.2 Å, while at the closer carbon center a carbene structure is already forming. One interesting structural feature of $TSCH_4$ is that Nb atom participates to some extent to the hydrogen migration process lowering the activation barrier as documented by the short Nb–H distance (1.797 Å compares well with 1.731 Å for the Nb–H in triplet $H–Nb–C_2H_5$ complex). The quintet $TSCH_4$ is by 1.20 eV higher in energy and does not profit from this extra stabilization.

Reductive elimination of methane and formation of $Nb–CH_2^+$ is a barrierless process, with reaction products situated 0.23 eV below the reactants asymptote.

From the $CH_3–Nb^+–CH_3$ intermediate through direct bond cleavage of one of the Nb–C bonds the $NbCH_3^+ + CH_3$ products can be obtained and Fig. 3 shows that this process is calculated to be endothermic by 1.25 eV. The experimentally measured threshold for this fragmentation process is 1.67 ± 0.07 eV [21], again higher than the presently predicted value. Since direct formation of $NbCH_3^+ + CH_3$ products, although entropically favoured, appears to be energetically much more demanding than the tight $TSCH_4$ transition state for the 1,3 hydrogen shift high kinetic energies are required for the process to occur.

Comparing the calculated PESs for the C–H and C–C activation branches, we can summarize the results as follows. Both hydrogen and methane elimination reactions are initiated by the formation of a quintet $Nb(C_2H_6)^+$ ion-molecule complex. Due to the lower stability of the quintet C–H and C–C insertion intermediates relative to their triplet counterparts a crossing occurs in both cases and the reactions proceed on the low-spin surfaces. The overall H_2 elimination reaction is calculated to be exothermic by 0.23 eV and the highest energy point en route to the products is the C–H insertion TS that has been located 0.13 eV below the entrance channel. Owing to the characteristics of the C–H insertion TS, the direct bond breaking processes from the common intermediate $H–Nb^+–C_2H_5$ to obtain NbH^+ and $NbC_2H_5^+$ fragments are not energetically competitive although entropically favored.

The overall methane elimination reaction is predicted to be exothermic by 0.23 eV. Even if the C–C insertion $CH_3–Nb^+–CH_3$ product is a very low energy intermediate, the C–C insertion TS barrier exceeds the energy of the ground state reactants by 0.58 eV and prevents observation of this species under thermal conditions. From this dimethyl insertion intermediate the reaction can proceed to give methane loss products or, alternatively, $NbCH_3^+ + CH_3$ products by direct bond cleavage with a net energy requirement of 1.25 eV.

3.3 Bond energies

Armentrout and co-workers [21] have reexamined niobium hydrogen and niobium carbon bond dissociation energies for the fragments relevant to the ethane activation reaction mediated by bare niobium cation. Mainly with these updated values and with former theoretical [25–34] and experimental [22–24] predictions are compared thermochemical data calculated by us and reported in Table 1. The most relevant structural information concerning ground state geometries of $Nb^+–H$ and $Nb^+–R$ fragments can be found in Fig. 5. At a first glance, from inspection of Table 1, it appears that there is a general fairly good agreement between theory and experiment with some exceptions.

The predicted value of the NbH^+BDE is in very good agreement with experimental determination, the difference being less than 0.1 eV.

To calculate the BDE for $Nb–2H^+$ it is necessary to individuate the structure of the complex which the dissociation occurs from. On the basis of our results, the $Nb(H_2)^+$ fragment can be formed only from the $(H_2)Nb^+–C_2H_4$ insertion intermediate by direct barrierless cleavage of the Nb–C bond and loss of ethylene. However, we have also examined the possibility that the electrostatic complex, $Nb(H_2)^+$, could rearrange to give a dihydrido covalently bound complex, NbH_2^+. The ground state of the NbH_2^+ complex is $^3A'$, with a HNbH angle of 112°, that is less stable than the quintet $Nb(H_2)^+$ ground state by about 0.52 eV. Thus, the BDE value of 5.05 eV, reported in Table 1, has been calculated for the dissociation from the $Nb(H_2)^+$ electrostatic complex. The BDE calculated by us compares well with the former experimentally estimated value of 5.15 eV [23], while it is overestimated by 0.41 eV with respect to the value suggested by Armentrout.

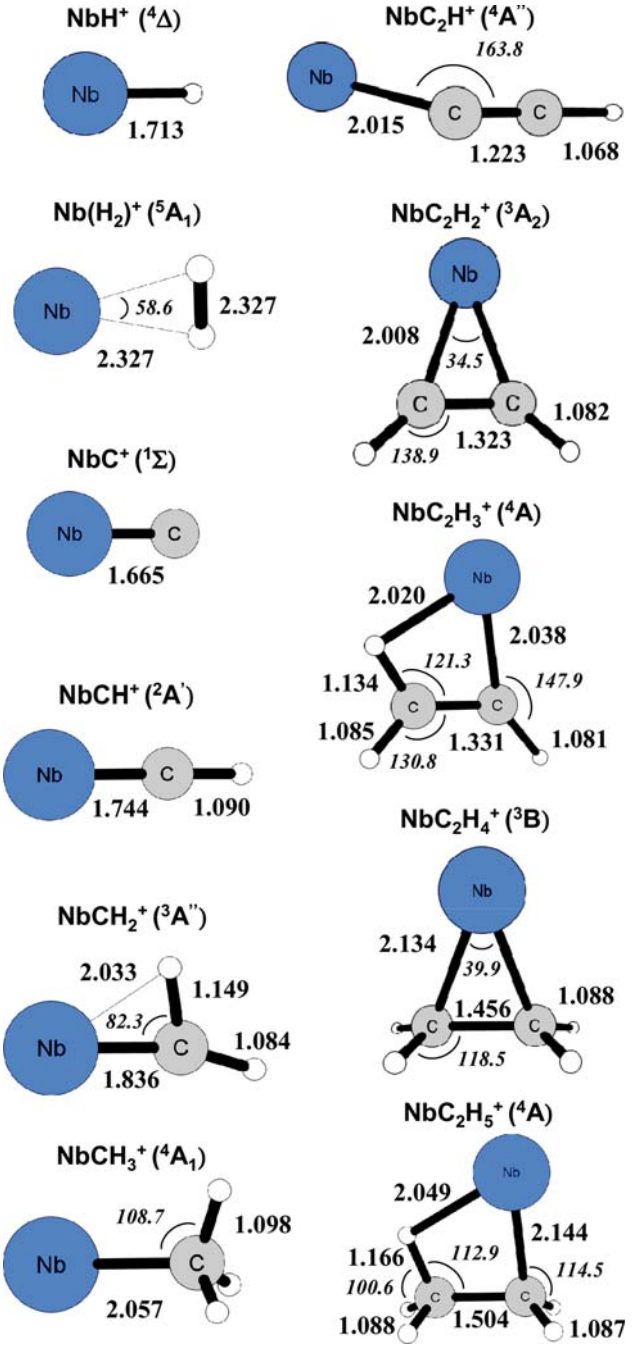

Fig. 5 Geometrical parameters of ground states structures of some cationic fragments relevant to the ethane activation by Nb^+. Bond lengths are in angstroms and angles in degrees

For the triple Nb–C bond of the NbC^+ fragment we propose a binding energy of 4.55 eV. This value is underestimated in comparison with the best available experimental estimate of 5.28 eV that, however could be improved owing to the uncertainties of the experimental determination [21].

The agreement improves for the next three $NbCH^+$, $NbCH_2^+$ and $NbCH_3^+$ fragments. As shown in Table 1, the experimental values exceed the calculated BDEs by 0.45 and 0.32 eV for $NbCH^+$ and $NbCH_2^+$, respectively. The value of 4.12 eV proposed by us for $NbCH_2^+$ is the same of that calculated by Siegbahn et al. [28]. The theoretical value of 2.31 eV for the $NbCH_3^+$ BDE is overestimated by 0.25 eV in comparison with the experimental one.

As discussed by Armentrout et al., the BDE of the $NbC_2H_3^+$ fragment is less than that of a Nb–C double bond, as in $NbCH_2^+$, but greater than that of a single Nb–C bond, as in $NbCH_3^+$. The enhancement calculated here is of 1.04 eV. NBO analysis confirms that there is an extra stabilization due to back-donation of the C–C π electrons to the metal center. In addition, a sort of β-agostic interaction between one C–H bond of the CH_2 group and the niobium atom, evidenced by the elongation of the C–H bond and the reduction of the HCC bond angle (see Fig. 5), further contributes to this enhancement. We have estimated that back-donation and agostic interaction amount to about 0.8 and 0.25 eV, respectively.

The value of the binding energy for the $NbC_2H_5^+$ fragment is overestimated by 0.19 eV with respect to the value suggested by Armentrout of 2.45 ± 0.12 eV [21]. As can be deduced from geometrical data in Fig. 5, the same kind of β-agostic stabilization due the interaction between the niobium center and one C–H bond of the methyl group, exists also in $NbC_2H_5^+$. The BDE value calculated by us is 2.64 eV, that is 0.36 eV (0.38 eV is the difference between experimental values) greater than Nb^+–CH_3 BDE. The energy stabilization associated with this interaction has been estimated eliminating the interaction through rotation of the methyl group. Therefore, including the energy for the conformational change (0.12 eV for CH_3–CH_3), the energy stabilization with respect to the structure with no agostic interaction has been calculated as 0.26 eV.

The calculated BDE for NbC_2H^+ is 4.72 eV, that is 0.38 eV greater than the experimental value of 4.34 ± 0.19 eV. As can be inferred from the geometrical parameters reported in Fig. 5 and from the NBO analysis, this species has a Nb–C≡C–H structure. However, the strength of the Nb–C bond is comparable to that of the double bond in Nb^+–CH_2. The NBO second-order perturbation analysis gives two consistent energy stabilization contributions due to the delocalization of both pairs of C–C π electrons into the $d\pi$ orbitals of niobium.

Finally, we discuss the theoretical BDEs obtained for the $NbC_2H_2^+$ and $NbC_2H_4^+$ species. The BDE value of 2.58 eV calculated for $NbC_2H_2^+$ is underestimated by 0.32 eV with respect to that suggested by Armentrout, but it is very close, instead, to the previously measured [23] and calculated [34] values of 2.47 ± 0.13 and 2.56 eV, respectively. For $NbC_2H_4^+$ our calculations give a value of 1.53 eV that is about half of the experimental value measured to be 2.80 ± 0.30 eV. The calculated difference in binding energy between the two $NbC_2H_4^+$ and $NbC_2H_2^+$ fragments is in agreement with the

Table 1 Calculated BDEs (in eV) compared with experimental and previous theoretical determinations

Species	BDE	Exp[a]	Exp	Theory
Nb^+–H	2.36	–	2.28 (0.07)[b]	2.11[e], 2.28[f], 2.34[g], 2.45[i], 2.55[j], 2.56[h]
Nb^+–2H	5.05	4.64 (0.06)	5.15 (0.04)[c]	4.14[k]
Nb^+–C	4.55	5.28 (0.15)	5.16 (0.15)[b]	–
Nb^+–CH	5.57	6.02 (0.20)	6.29 (0.35)[d]	–
Nb^+–CH_2	4.12	4.44 (0.09)	4.60 (0.30)[d]	3.86[l], 4.12[i]
Nb^+–CH_3	2.31	2.06 (0.11)	–	2.15 (0.13)[j]
Nb^+–C_2H	4.72	4.34 (0.19)	–	–
Nb^+–C_2H_2	2.58	2.90 (0.06)	2.47 (0.13)[c]	2.56 (0.13)[m]
Nb^+–C_2H_3	3.35	3.43 (0.21)	–	–
Nb^+–C_2H_4	1.53	2.80 (0.30)	–	–
Nb^+–C_2H_5	2.64	2.45 (0.12)	–	–

[a] Ref. [21]
[b] Ref. [22]
[c] Ref. [23], both experimental and calculated BDE for this species refer to dissociation from the electrostatic complex $Nb(H_2)^+$
[d] Ref. [24]
[e] Ref. [25]
[f] Ref. [26]
[g] Ref. [27]
[h] Ref. [28]
[i] Ref. [32]
[j] Ref. [29]
[k] Ref. [31]
[l] Ref. [30]
[m] Ref. [34]

trends reported for the left first-row transition metal cations [50] and can be analogously ascribed to the weaker π bond of acetylene. Indeed, the bonding situation in transition metal complexes with alkenes or alkynes as π-bonded ligands is usually discussed within the framework of the Dewar–Chatt–Duncanson (DCD) model [51,52]. The bonding arises through a synergistic ligand-to-metal σ-donation from the occupied in-plane π-orbitals of the alkene/alkyne into the empty *d* orbitals of the metal, and metal-to-ligand π-back-donation from the occupied *d* orbitals of the metal into the empty π* orbital of the ligand. An extreme version of the same bonding model considers the alkene/alkyne complex as a metallacyclic compound in which the metal–ligand interactions are described in terms of two electron sharing σ-bonds between the metal and the carbon atoms. The definitive breaking of the π bond can be monitored by the elongation of the C–C bond with respect to free ligand molecules and the partial pyramidalization (ethylene ligand) or bending (acetylene ligand) at the carbon bonds. From Fig. 5 it can be deduced that the geometrical parameters of the interacting ethylene and acetylene molecules are significantly modified with respect to the gas-phase values. The elongation of the C–C bond and the deformation of the C–C–H bond angles of the acetylene molecule clearly indicate that a metallacyclic compound is formed, as it is confirmed by the NBO analysis. Therefore, the actual difference between the predicted binding energies of $NbC_2H_2^+$ and $NbC_2H_4^+$ arises from the different strengths of the π bonds that it is necessary to break. Indeed, it requires more energy to break the π C–C bond in ethylene than that in acetylene. However, an additional strain for the metal–acetylene cation, arising from the shorter C–C bond length, results in the final computed difference of 1.05 eV between the BDEs of $NbC_2H_2^+$ and $NbC_2H_4^+$.

4 Conclusions

The present paper deals with the ethane C–H and C–C bond activation mediated by high- and low-spin states of bare Nb cation. Potential energy surfaces have been investigated in detail at the B3LYP level of theory and minima and transition states have been localized and characterized. Comparison between the pathways for C–H and C–C activation branches shows that after formation of a common ion-molecule adduct at the entrance channel of the reaction, both activation processes proceed to give an insertion intermediate via oxidative addition. In both cases, the step corresponding to insertion into the C–H and C–C bond, respectively, is energetically more demanding than the subsequent ones. However, the triplet transition state for the C–H insertion lies very low in

energy, by 0.13 eV below the reactants dissociation asymptote, and the associated barrier is 0.81 eV high. On the contrary, the relative energy of the quintet transition state for the C–C insertion, calculated respect to ground state reactants, is 0.58 eV and the barrier is 1.52 eV. Due to the change of insertion intermediates spin multiplicity with respect to ground state reactants dissociation limit, a spin crossing has to occur, for both processes, in the region of the insertion transition states. The overall hydrogen elimination reaction, as a result of the Nb^+ insertion into C–H, and the methane loss, as a result of the Nb^+ insertion into C–C bond, are found to be exothermic by 0.23 eV. Alternative fragmentation pathways, going through direct bond cleavage, appear to become competitive only at significantly higher kinetic energies. Calculated niobium-hydrogen and niobium-carbon bond dissociation energies for cationic fragments relevant to the ethane activation are in fairly good agreement with experimental values with some exceptions that have been commented.

Acknowledgments Financial support from the Università degli Studi della Calabria and MIUR is gratefully acknowledged.

References

1. Arakawa H, Aresta M, Armor JN, Barteau MA, Beckman EJ, Bell AT, Bercaw JE, Creutz C, Dinjus E, Dixon DA, Domen K, DuBois DL, Eckert J, Fujita E, Gibson DH, Goddard WA, Goodman DW, Keller J, Kubas GJ, Kung HH, Lyons JE, Manzer LE, Marks TJ, Morokuma K, Nicholas KM, Periana R, Que L, Rostrup-Nielson J, Sachtler WMH, Schmidt LD, Sen A, Somorjai GA, Stair PC, Stults BR, Tumas W (2001) Chem Rev 101:953
2. Crabtree RH (2001) J Chem Soc Dalton Trans 2437
3. Labinger JA, Bercaw JE (2002) Nature 417:507
4. Schwarz H (2004) Int J Mass Spectrom 237:75 and references therein
5. Chen X, Feng X, Wang Y, Wang T, Liu X, Zheng X (2007) Chem Phys Lett 443:430
6. Gracia L, Sambrano JR, Safont VS, Calatayud M, Beltrán A, Andrés J (2003) J Phys Chem A 107:3107
7. Rivalta I, Russo N, Sicilia E (2006) J Comput Chem 27:174
8. Armentrout PB, Beauchamp JL (1989) Acc Chem Res 22:315
9. Armentrout PB (1991) Science 251:175
10. Schröder D, Shaik S, Schwarz H (2000) Acc Chem Res 33:139
11. Poli R, Harvey JN (2003) Chem Soc Rev 32:1
12. Poli R (2004) J Organomet Chem 689:4291
13. Harvey JN (2007) Phys Chem Chem Phys 9:331
14. Russo N, Sicilia E (2001) J Am Chem Soc 123:2588
15. Russo N, Sicilia E (2002) J Am Chem Soc 124:1471
16. Michelini MC, Russo N, Sicilia E (2002) J Phys Chem 106:8937
17. Michelini MC, Russo N, Sicilia E (2004) Inorg Chem 43:4944
18. Chiodo S, Kondakova O, Irigoras A, Michelini MC, Russo N, Sicilia E, Ugalde JM (2004) J Phys Chem A 108:1069
19. Rivalta I, Russo N, Sicilia E (2006) J Mol Struct (THEOCHEM) 762:25
20. Martinez M, Michelini MC, Rivalta I, Russo N, Sicilia E (2005) Inorg Chem 44:9807
21. Sievers MR, Chen Y-M, Haynes CL, Armentrout PB (2000) Int J Mass Spectrom 195/196:149
22. Sievers MR, Chen Y-M, Armentrout PB (1996) J Chem Phys 100:54
23. Ranatunga DRA, Freiser BS (1995) Chem Phys Lett 233:319
24. Hettich RL, Freiser BS (1987) J Am Chem Soc 109:3543
25. Schilling JB, Goddard III WA, Beauchamp JL (1987) J Am Chem Soc 109:5565
26. Pettersson LGM, Bauschlicher CW Jr, Langhoff SR, Partridge H (1987) J Chem Phys 87:481
27. Das KK, Balasubramanian K (1991) J Mol Spectrosc 148:250
28. Siegbahn PEM, Blomberg MRA, Svensson M (1994) Chem Phys Lett 223:35
29. Das KK, Balasubramanian K (1990) J Mol Spectrosc 144:245
30. Bauschlicher CW Jr, Partridge H, Sheehy JA, Langhoff SR, Rosi M (1992) J Phys Chem 96:6969
31. Das KK, Balasubramanian K (1989) J Chem Phys 91:6254
32. Bauschlicher CW Jr, Langhoff SR, Partridge H, Barnes LA (1989) J Chem Phys 91:2399
33. Rosi M, Bauschlicher CW Jr, Langhoff SR, Partridge H (1990) J Phys Chem 94:8656
34. Sodupe M, Bauschlicher CW Jr (1991) J Phys Chem 95:8640
35. Becke AD (1993) J Chem Phys 98:5648
36. Stephens PJ, Devlin FJ, Chabalowski CF, Frisch MJ (1994) J Phys Chem 98:11623
37. Frisch MJ, Trucks GW, Schlegel HB, Scuseria GE, Robb MA, Cheeseman JR, Montgomery JA Jr, Vreven T, Kudin KN, Burant JC, Millam JM, Iyengar SS, Tomasi J, Barone V, Mennucci B, Cossi M, Scalmani G, Rega N, Petersson GA, Nakatsuji H, Hada M, Ehara M, Toyota K, Fukuda R, Hasegawa J, Ishida M, Nakajima T, Honda Y, Kitao O, Nakai H, Klene M, Li X, Knox JE, Hratchian HP, Cross JB, Bakken V, Adamo C, Jaramillo J, Gomperts R, Stratmann RE, Yazyev O, Austin AJ, Cammi R, Pomelli C, Ochterski JW, Ayala PY, Morokuma K, Voth GA, Salvador P, Dannenberg JJ, Zakrzewski VG, Dapprich S, Daniels AD, Strain MC, Farkas O, Malick DK, Rabuck AD, Raghavachari K, Foresman JB, Ortiz JV, Cui Q, Baboul AG, Clifford S, Cioslowski J, Stefanov BB, Liu G, Liashenko A, Piskorz P, Komaromi I, Martin RL, Fox DJ, Keith T, Al-Laham MA, Peng CY, Nanayakkara A, Challacombe M, Gill PMW, Johnson B, Chen W, Wong MW, Gonzalez C, Pople JA (2004). Gaussian, Wallingford
38. Hay P J, Wadt WR (1985) J Chem Phys 82:270
39. Hay PJ, Wadt WR (1985) J Chem Phys 82:284
40. Hay PJ, Wadt WR (1985) J Chem Phys 82:299
41. Krishnan R, Binkley JS, Seeger R, Pople JA (1980) J Chem Phys 72:650
42. Blaudeau JP, McGrath MP, Curtis LA, Radom LJ (1997) Chem Phys 107:5016
43. Gonzales C, Schlegel HB (1989) J Chem Phys 90:2154
44. Gonzales C, Schlegel HB (1990) J Phys Chem 94:5523
45. Boys SB, Bernardi F (1970) Mol Phys 19:553
46. Carpenter JE, Weinhold F (1988) J Mol Struct. (THEOCHEM) 169:41
47. Carpenter JE, Weinhold FJ (1988) The structure of small molecules and ions. Plenum, New York
48. Buckner SW, MacMahon TJ, Byrd GD, Freiser BS (1989) Inorg Chem 28:3511
49. Moore CE (1991) Atomic energy levels. NSRD-NBS, USA. vol 1. US Government Printing Office, Washington
50. Sodupe M, Bauschlicher CW Jr, Langhoff SR, Partridge H (1991) J Phys Chem 96:2118
51. Dewar MJS (1951) Bull Soc Chim Fr 79
52. Chatt J, Duncanson LA (1953) J Chem Soc 2939